THE JOURNAL OF BIOLOGICAL CHEMISTRY VOL. 287, NO. 20, pp. 16346–16355, May 11, 2012
Published in the U.S.A.

NMR Studies of Hexaacylated Endotoxin Bound to Wild-type and F126A Mutant MD-2 and MD-2·TLR4 Ectodomain Complexes*[S]

Received for publication, January 17, 2012, and in revised form, March 12, 2012 Published, JBC Papers in Press, March 20, 2012, DOI 10.1074/jbc.M112.343467

Liping Yu[‡§], Rachel L. Phillips[¶], DeSheng Zhang[¶], Athmane Teghanemt[¶], Jerrold P. Weiss[¶‖], and Theresa L. Gioannini[§¶1]**

From the [‡]NMR Core Facility, [§]Department of Biochemistry, [¶]Inflammation Program, Department of Internal Medicine, and [‖]Department of Microbiology, Roy A. and Lucille J. Carver College of Medicine, University of Iowa, Iowa City, Iowa 52241, and the [**]Department of Veterans' Affairs Medical Center, Iowa City, Iowa 52246

Background: Phenylalanine 126 of MD-2 is essential for endotoxin-induced TLR4 activation.
Results: NMR of ^{13}C-labeled endotoxin bound to wt or F126A MD-2 ± TLR4 ectodomain reveals effects of Phe^{126} on interactions of MD-2 ± TLR4 with endotoxin.
Conclusion: Phe^{126} acts as a "hydrophobic switch" promoting agonist-dependent TLR4 dimerization.
Significance: This study describes a novel approach to further define the structural requirements for endotoxin-induced TLR4 activation.

Host response to invasion by many Gram-negative bacteria depends upon activation of Toll-like receptor 4 (TLR4) by endotoxin presented as a monomer bound to myeloid differentiation factor 2 (MD-2). Metabolic labeling of hexaacylated endotoxin (LOS) from *Neisseria meningitidis* with [^{13}C]acetate allowed the use of NMR to examine structural properties of the fatty acyl chains of LOS present in TLR4-agonistic and -antagonistic binary and ternary complexes with, respectively, wild-type or mutant (F126A) MD-2 ± TLR4 ectodomain. Chemical shift perturbation indicates that Phe^{126} affects the environment and/or position of each of the bound fatty acyl chains both in the binary LOS·MD-2 complex and in the ternary LOS·MD-2·TLR4 ectodomain complex. In both wild-type and mutant LOS·MD-2 complexes, one of the six fatty acyl chains of LOS is more susceptible to paramagnetic attenuation, suggesting protrusion of that fatty acyl chain from the hydrophobic pocket of MD-2, independent of association with TLR4. These findings indicate that re-orientation of the aromatic side chain of Phe^{126} is induced by binding of hexaacylated E, preceding interaction with TLR4. This re-arrangement of Phe^{126} may act as a "hydrophobic switch," driving agonist-dependent contacts needed for TLR4 dimerization and activation.

Recognition of endotoxin (E),[2] unique glycolipids present on the surface of Gram-negative bacteria (GNB), is pivotal for host responses to many GNB (1, 2). The ability to respond to minute (pM) concentrations of E depends on the ordered action of four extracellular and cell surface host proteins: lipopolysaccharide-binding protein (LBP), soluble (s) and GPI-linked membrane (m)-associated forms of CD14, secreted and TLR4-associated MD-2 and TLR4 (1, 3–5). Among the various TLRs, TLR4 plays the major role in recognition and response to E and is unique in that its activation leads to both MyD88-dependent (NFκB-mediated) and TRIF-dependent (interferon-mediated) cellular responses (6–11). The concerted action of LBP, CD14 and MD-2 dramatically alters the physical presentation of E, such that individual E monomers are extracted from GNB or purified E aggregates to form monomeric E·protein complexes that, at pM E concentrations, indirectly (E·CD14 with MD-2·TLR4) or directly (E·MD-2 with TLR4) engage TLR4 and cause receptor and cell activation (3, 12–14).

Recent biochemical and structural studies have significantly advanced understanding of the molecular and structural basis of ligand-receptor interaction, and how this interaction results in TLR4 activation (3, 12–17). MD-2 forms a heterodimer with TLR4 by agonist-independent binding to sites within the N-terminal and central leucine-rich repeat (LRR) domains of the TLR4 ectodomain (TLR4ecd) (15, 17). Comparison of the published crystal structures of MD-2 bound to TLR4 antagonists (lipid IVA and eritoran) to that of the agonist-driven heteroligomer, $[TLR4ecd{\cdot}MD\text{-}2{\cdot}LPS]_2$ has revealed that binding of TLR4-activating LPS to MD-2 induces additional agonist-dependent contacts of MD-2 and LPS with TLR4 involving sites within the C-terminal LRR domain of the ectodomain of a second TLR4 molecule (15–17). When tetraacylated antagonists, such as lipid IVA and eritoran, are bound to MD-2, each of the four tightly packed fatty acyl chains fits within the deep, hydrophobic cavity of MD-2 and is protected from the aqueous solvent (15, 16). In contrast, when hexaacylated LPS is bound to the MD-2·TLR4ecd heterodimer, the tail of one fatty acyl chain of LPS protrudes from the pocket of MD-2 of one ternary com-

* This work was supported, in whole or in part, by grants from the Dept. of Veterans' Affairs, Merit Grant (to T. L. G.) and from NIAID, National Institutes of Health Grant AI05732 (to J. P. W.).
[S] This article contains supplemental Table S1 and Figs. S1–S3.
[1] To whom correspondence should be addressed: The Dept. of Veterans' Affairs Medical Center, Iowa City, IA 52246, and the Inflammation Program, Dept. of Internal Medicine, Roy A. and Lucille J. Carver College of Medicine, University of Iowa, 2501 Crosspark Rd, Coralville, IA 52241. Tel.: 319-335-4253; Fax: 319-335-4194; E-mail: theresa-gioannini@uiowa.edu.
[2] The abbreviations used are: E, endotoxin; E·albumin, endotoxin·albumin; LOS, lipooligosaccharide; MD-2, myeloid differentiation factor 2; PRE, paramagnetic relaxation enhancement; TLR4, Toll-like receptor 4; TLR4ecd, TLR4 ectodomain.

plex leading to contacts between this fatty acyl chain and TLR4ecd of a second ternary complex (15, 17).

An apparently critical determinant for agonist (*i.e.* hexaacylated lipid A/endotoxin)-dependent activation of TLR4 is the presence of an aromatic or hydrophobic amino acid, most often phenylalanine 126, at the mouth of the hydrophobic cavity of MD-2 (18–20). F126A mutants of both human and murine MD-2 do not support endotoxin-dependent activation of TLR4 (21–23). Monomeric complexes of endotoxin·human (h)MD-2 wild-type (wt) and endotoxin·hMD-2 F126A display the same high affinity ($K_d \sim 100-200$ pM) for TLR4, but the mutant complex has ≤ 1% the TLR4 agonist activity of the wt complex and is a TLR4 antagonist (12, 13, 22). Phe^{126} in hMD-2 clearly plays an essential role in agonist-dependent contacts between two ligand·MD-2·TLR4 ternary complexes. Comparison of the crystal structures of MD-2 complexed with non-activating ligands (lipid IVA, eritoran, myristic acid) with the crystal structure of [TLR4ecd·MD-2·LPS]$_2$ revealed a re-arrangement of the Phe^{126}-containing loop ("Phe^{126} loop") of MD-2 apparently driven by re-orientation of the Phe^{126} aromatic side chain from outside the pocket when bound to a non-activating ligand, to inward toward the hydrophobic cavity when activating hexaacylated LPS was bound (15–17). As suggested by Park *et al.* (17), this local conformational re-arrangement in MD-2 involving Phe^{126} could be critical for LPS-triggered TLR4 activation by influencing the position of the fatty acyl chains of bound activating LPS and fatty acyl:TLR4 contacts that drive TLR4 dimerization and activation. In addition, the re-arrangement of the Phe^{126} loop could promote MD-2:TLR4 contacts at the dimerization interface.

Because the structure of a potent TLR4-activating endotoxin bound to MD-2 in the absence of TLR4 has not been reported, it is not known whether the inability of the fatty acyl chains of hexaacylated agonist lipid A to fit completely into the MD-2 pocket helps drive dimerization of LPS·MD-2·TLR4 or whether contact with the second TLR4 stabilizes the extrusion of the sixth fatty acyl chain and subsequent conformational changes in MD-2. It also is not clear if agonist-induced re-orientation of Phe^{126} in MD-2 is triggered by the binding of a TLR4-activating lipid A/endotoxin to MD-2 independent of TLR4 or if binding to TLR4 is required to stabilize this altered conformation.

We now report NMR studies of the acyl chain properties of hexaacylated endotoxin bound to wt or mutant F126A hMD-2 and as part of a monomeric ternary complex of E·MD-2, wt or F126A·TLR4ecd. These studies were designed to address two questions: 1) Are protrusion of a single fatty acyl chain and re-orientation of the aromatic side chain of Phe^{126} intrinsic properties of TLR4-activating hexaacylated E·MD-2 complexes induced before contact with TLR4? 2) Does Phe^{126} of MD-2 affect positioning of the acyl chains of bound hexaacylated E that may drive contacts with TLR4 at the dimerization interface leading to TLR4 activation? Key to these studies was our ability to metabolically label uniformly and efficiently the acyl chains of endotoxin with alternating [^{13}C] and [^{12}C] atoms and generate mg quantities of purified monomeric, functional, and stable endotoxin·MD-2, TLR4ecd, and endotoxin·MD-2 wt and F126A·TLR4ecd complexes. Results of the NMR studies indicate that protrusion of one of the six fatty acyl chains of endotoxin bound to MD-2 precedes interaction with TLR4 when endotoxin is bound to either wt or F126A MD-2. Consequently, the presence of a protruding fatty acyl chain is not a distinguishing feature of TLR4-activating E·MD-2 complexes and so is not sufficient for driving TLR4 activation. However, the position and surrounding environment of the bound fatty acyl chains in MD-2 are altered when Phe^{126} is substituted with alanine. In the endotoxin·MD-2 wt complex, the aromatic side chain of Phe^{126} is re-oriented toward the hydrophobic cavity preceding interaction with TLR4. Local rearrangements of the Phe^{126} loop in MD-2 may promote TLR4 dimerization and activation, by affecting both contacts between the protruded fatty acyl chain and TLR4 as well as MD-2:TLR4 contacts.

EXPERIMENTAL PROCEDURES

Materials—Metabolically labeled [$^{13/14}$C]LOS endotoxin was isolated from NMB Ace1 grown in Morse medium supplemented with 2 mM 1-[^{12}C],2-[^{13}C]acetate (Moravek Chemicals, Brea, CA) and 1 uCi/ml of 1,2-[^{14}C]acetate as previously described (24, 25). [$^{13/14}$C]LOS contained alternating [^{13}C] and [^{12}C]carbon atoms starting with the [^{13}C] terminal methyl in each fatty acyl chain of LOS (Fig. 2*D*) and had sufficient radioactivity (15 cpm/pmol LOS) to monitor purification and facilitate quantitative analysis. To minimize effects of possible endotoxin heterogeneity, a single preparation of purified [$^{13/14}$C]-LOS was used. [^{3}H]LOS·MD-2 (25,000 cpm/pmol) was prepared as described (13, 24). Reagents used include: human serum albumin (HSA), an endotoxin-free, 25% stock solution (Baxter Health Care, Glendale, CA), bovine serum albumin (BSA), and other chemical reagents from Sigma, and chromatography matrices (GE Healthcare, Piscataway, NJ). Purified Gd(DPTA-BMA) was a gift from Dr. Klaus Zangger, University of Graz, Graz, Austria.

Production of Recombinant WT and F126A hMD-2 and TLR4 Ectodomain—As previously described (12, 13), cDNA encoding human MD-2 wt, F126A, or TLR4 ectodomain, amino acids 24–631, was inserted using SacII and XhoI restriction sites into pBAC3 (Novagen) that provides secreted proteins with a six-residue polyhistidine tag at the N terminus. Baculoviral stocks, generated by transfection of BacVec3000 (Novagen) and plasmid and then amplified in Sf9 cells, were used to infect High Five™ (Invitrogen) insect cells for protein production. Large scale (20 liters) preparations of conditioned insect medium containing MD-2 (wt or F126A) or TLR4ecd were produced by BlueSky Biotech, Worcester, MA. Recombinant proteins in conditioned media were stable at −80 °C.

Preparation of LOS·MD-2 Complexes—[$^{13/14}$C]LOS·albumin complexes were generated and purified from [$^{13/14}$C]LOS aggregates solubilized in buffer A (100 mM Tris-HCl 5 mM EDTA, pH 8.0) as previously described (26). LOS·albumin complexes (1 mg LOS, 30 ml) were diluted 10-fold with buffer A and incubated with 2 liters of conditioned insect medium containing His$_6$-sMD-2, wt or F126A (~1 μg/ml active, monomeric sMD-2) for 3 h at 37 °C. An aliquot of the reaction mixture was analyzed on Sephacryl S200 to measure generation of [$^{13/14}$C]-LOS·MD-2. The reaction mixture was dialyzed (Spectrapor1) against buffer B (20 mM phosphate, 0.5 M NaCl, 5 mM imidazole, pH 7.6) and loaded onto Ni FF Sepharose (5 cm × 25 cm) at 4 °C

at a flow rate of 3 ml/min (GE Healthcare Explorer FPLC). After washing the column with 20 mM imidazole in buffer B, the adsorbed material was eluted by an imidazole gradient in buffer B. Gradient fractions containing radioactive LOS were combined, concentrated to ~2 ml (Millipore Centriplus-70), and applied to Sephacryl S100 (1.6 × 100 cm) equilibrated in buffer C (20 mM phosphate, 150 mM NaCl, pH 7.1). Radioactive fractions consistent with the M_r of LOS·MD-2 were combined and concentrated to ~1 ml (Millipore Centricon MWCO 10K). Purity of the samples was confirmed by Coomassie Blue stain of 10–15% gradient PhastGels (GE Healthcare). Each LOS·MD-2 complex analyzed by NMR was derived from reactions of 12–14 liters of conditioned medium containing MD-2. The final samples (1 ml) contained 240 and 260 μM of LOS·MD-2 wt and F126A, respectively. [^{12}C]LOS·MD-2 was prepared by the identical procedure described above.

The functional activity of purified LOS·MD-2 complexes was measured by TLR4-dependent cell activation. HEK293 cells, parent, or TLR4-containing, were seeded in a 96-well plate (1 × 10^5 cells/well) in DMEM/10% FBS and incubated overnight at 37 °C in 5% CO_2/95% humidity. The next day, cells were washed twice with PBS, pH 7.4. Increasing doses of purified LOS·MD-2 wt and F126A were added in 200 μl of DMEM/0.1% HSA. After 18 h at 37 °C, cell supernatants were collected and tested for accumulation of extracellular IL-8 by ELISA (BD Biosciences).

Preparation of His_6-TLR4ecd and LOS·MD-2·HisTLR4ecd Complexes—Conditioned insect cell medium (2–3 liters) containing His_6-TLR4ecd was dialyzed overnight against buffer B at 4 °C and then applied to Ni FF Sepharose (5 × 30 cm) equilibrated in buffer B at 4 °C (3 ml/min flow rate). Adsorbed material was eluted as described above. Imidazole gradient fractions immunoreactive to an anti-His antibody (Qiagen) (27) were combined and concentrated (Centriplus-70). TLR4ecd preparations from 6–9 liters of conditioned medium were combined and further purified on Sephacryl S200 (1.6 × 100 cm) equilibrated in buffer D (20 mM phosphate, 150 mM NaCl, pH 7.1, 0.005% BSA). Fractions were tested by immunoblot (anti-His antibody) to identify the major immunopositive peak, estimated M_r ~75,000, *i.e.* the size for monomeric His_6-TLR4ecd. Purified TLR4ecd activity was tested by reaction with [^{3}H]LOS·MD-2 (25,000 cpm/pmol) followed by analysis of the products on Sephacryl S300 (1.6 cm × 70 cm) equilibrated in PBS, 0.1% HSA. Approximately 4.5 mg TLR4ecd derived from ~ 15 liters of conditioned insect medium was concentrated to 0.8 ml before reaction with each of the [$^{13/14}$C]-LOS·MD-2 complexes.

LOS·MD-2 wt and F126A complexes were separated from Gd(DPTA-BMA) used in PRE NMR experiments on Sephacryl S100. The purified LOS·MD-2 complexes were incubated with 1.2× molar excess of HisTLR4ecd in 900 μl for 30 min at 37 °C. An aliquot was analyzed on Sephacryl S300 to confirm complete conversion of [$^{13/14}$C]LOS·MD-2 complex to a ternary complex containing TLR4ecd.

NMR Spectroscopy—All NMR samples were exchanged into 10 mM sodium phosphate, pH 6.5, in 100% D_2O. The LOS·MD-2 complexes (~250 μM) were stable at 4 °C for at least 6 months as judged by NMR profile and size exclusion chromatography. Aliquots of the LOS·MD-2·TLR4ecd samples were chromatographed after NMR to check for stability.

NMR spectra were collected at 25 °C on a Bruker Avance II 800 MHz NMR spectrometer equipped with a sensitive TCI cyroprobe. High resolution ^{13}C/^{1}H HSQC spectra (28) of the $^{13}CH_3$ region were collected to provide maximal resolution of the individual LOS $^{13}CH_3$ groups. Relative solvent/surface exposure of individual LOS $^{13}CH_3$ groups in LOS·MD-2 complexes was examined using the PRE NMR method (29–31) by acquiring ^{1}H T_2 relaxation rates of the LOS $^{13}CH_3$ groups of the [^{13}C]LOS·MD-2 complexes in the absence and presence of a neutral chelating gadolinium paramagnetic agent Gd(DPTA-BMA), 2–16 mM, as previously described (29–31). The ^{1}H T_2 Carr-Purcell-Meiboom-Gill (CMPG) delays used in these experiments were 0.92, 14.71, and 27.58 ms. NMR spectra were processed with the NMRPipe package (32) and analyzed using NMRView software (33).

RESULTS

Production and Purification of [^{13}C]LOS·MD-2—To better define the effect of Phe^{126} of MD-2 on the positioning of the fatty acyl chains of bound hexaacylated endotoxin, we produced and purified [^{13}C]endotoxin·MD-2 complexes using wt and F126A hMD-2. Metabolic labeling of the endotoxin (lipooligosaccharide, LOS) of a *Neisseria meningitidis* serogroup B Ace1 mutant during growth in Morse medium supplemented with 2 mM 1-[^{12}C], 2-[^{13}C]acetate resulted in [^{13}C] labeling of alternating C atoms in each fatty acyl chain, starting with the terminal methyl group of each fatty acid. Trace amounts of [^{14}C]acetate (one part in 200 of [$^{12/13}$C]acetate) were added to the growth medium to yield sufficient radiolabeling of LOS (15 cpm/pmol) to facilitate quantitative monitoring of purification and recovery of desired products. All of the experiments described here were done with a single preparation of purified LOS to preclude sample-to-sample differences due to endotoxin heterogeneity.

Monomeric LOS·MD-2 complexes are most efficiently generated by LBP-catalyzed extraction and transfer of LOS monomers from LOS aggregates to sCD14 and subsequent transfer of monomeric LOS from sCD14 to (s)MD-2 (3, 12, 26). The amounts of [^{13}C]LOS·MD-2 needed for NMR analysis would have necessitated production of at least 25 mg of recombinant sCD14. Therefore, we took advantage of an alternative method we have recently developed for generation of LOS·MD-2 in high yield independent of (s)CD14 (26). This alternative method depends upon generation of monomeric endotoxin·albumin complexes during overnight incubation of E aggregates in a divalent cation-depleted environment supplemented with albumin. The resultant E·albumin complexes are efficient donors of E monomers to insect cell-derived His_6-MD-2 as needed for formation of monomeric E·MD-2 (26). Reaction of monomeric LOS·albumin complexes with insect cell conditioned medium containing His_6-MD-2 was followed by metal chelation chromatography (Fig. 1*A*) and size exclusion chromatography (Fig. 1*B*) to yield purified monomeric (Fig. 1, *B* and *C*), bioactive (Fig. 1*D*) LOS·MD-2; nearly 50% of LOS in the LOS·albumin complexes was recovered as LOS·MD-2. As seen in Fig. 1*A*, an imidazole gradient separated LOS·MD-2 from the

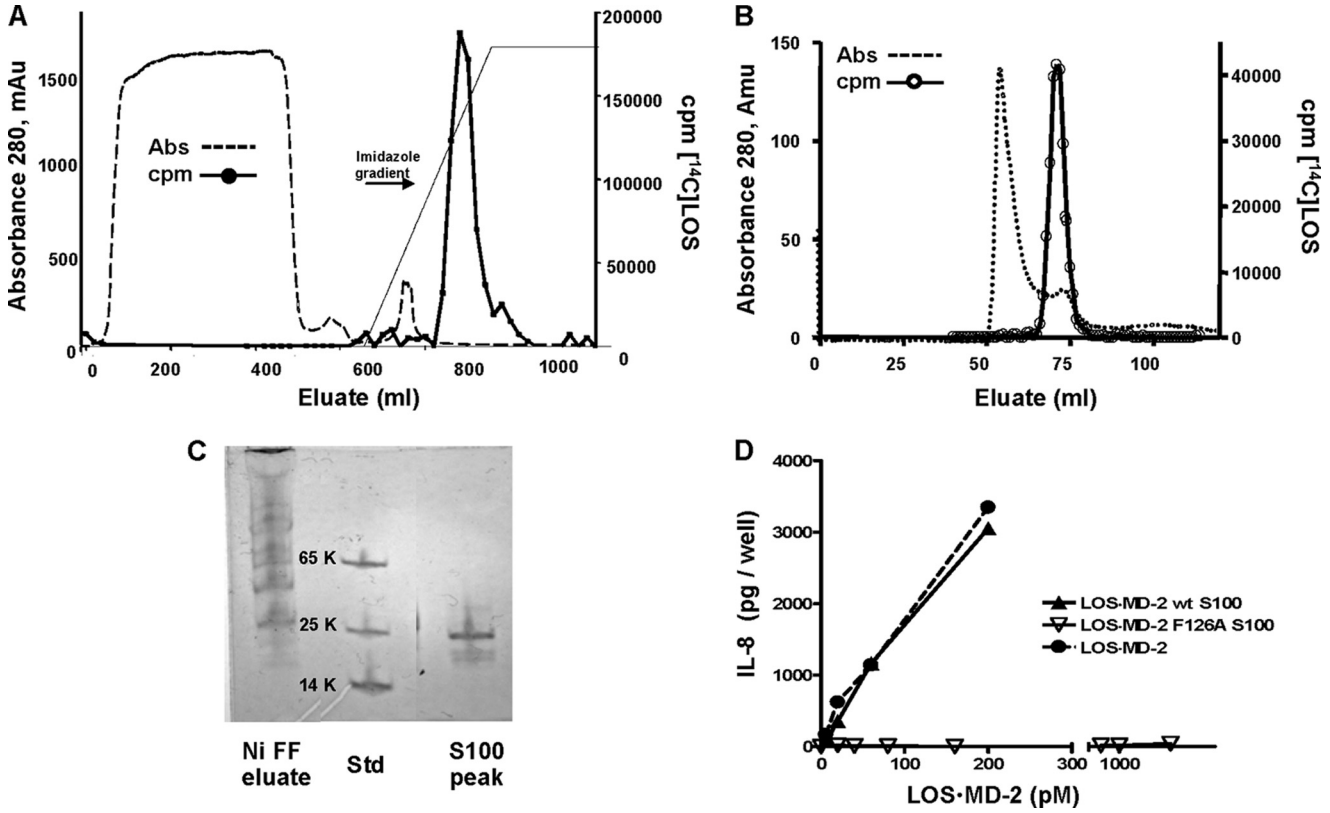

FIGURE 1. **Isolation and characterization of purified LOS·MD-2 complexes.** *A*, [13/14C]LOS·His_6MD-2 was isolated from Ni FF Sepharose by an imidazole gradient following the reaction of LOS·albumin (1 mg LOS) with conditioned insect medium containing sMD-2 (2 liters). The dialyzed reaction mixture was applied at 4 °C at a flow rate of 3 ml/min. (– – –), absorbance; (___) cpm [14C]LOS. *B*, radioactive peak containing [13/14C]LOS·His_6MD-2 recovered from an imidazole gradient from Ni FF Sepharose was concentrated and further purified by chromatography on Sephacryl S100 (1.6 cm × 100 cm) equilibrated in 20 mM phosphate, 150 mM NaCl, pH 7.1, (– – –), absorbance; (-○-) cpm [14C]LOS. *C*, imidazole eluate from Ni FF Sepharose (1 μl) and LOS·His_6MD-2 isolated from S100 and concentrated 10-fold (1 μl sample) were analyzed by PhastGel SDS-PAGE (10–15%)/Coomassie Blue stain. *D*, dose-dependent activation of HEK/TLR4 cells was measured by increasing concentrations of (-●-) [3H]LOS·His_6MD-2 (25,000 cpm/pmol), and purified [13/14C]LOS·His_6MD-2 wt (-▲-) and F126A (-△-). Cellular activation was monitored by accumulation of extracellular IL-8 determined by ELISA. IL-8 results shown are representative of at least two independent experiments, each sample performed in triplicate. The chromatographic profiles are representative of a typical purification experiment ($n > 5$); recovery of [14C]LOS was ≥80%.

bulk of insect protein(s) that also adhered to Ni FF-Sepharose. The identical procedure produced in similar yield and purity LOS·MD-2 F126A when insect cell conditioned medium containing His_6-MD-2 F126A was used. In contrast to LOS·MD-2 wt, the purified LOS·MD-2 F126A complex did not activate HEK/TLR4 cells (Fig. 1*D*) and acted as a TLR4 antagonist (data not shown).

NMR Analyses of WT and Mutant [13C]LOS·MD-2—High resolution $^{13}C/^{1}H$ HSQC spectra acquired on a 800 MHz NMR spectrometer for the $^{13}CH_3$ region of [13C]LOS complexed to wt and F126A MD-2 provided optimal resolution of the six acyl chain $^{13}CH_3$ groups (labeled as M1-M6) (Fig. 2, *A* and *B*). Interestingly, M1-M4 signals are clustered together, while M5 and M6 formed a separate cluster, reflecting the distinct local environment surrounding each $^{13}CH_3$ group of LOS when bound to MD-2. To ascertain that these crosspeaks were all derived from [13C]LOS and not from ^{13}C natural abundance signals of MD-2, [12C]LOS·MD-2 wt complex was prepared. NMR spectra collected under identical conditions for this control sample showed that there were virtually no detected crosspeaks in this region (data not shown), thus confirming that the observed signals in Fig. 2, *A* and *B* were derived specifically from the fatty acyl chains of [13C]LOS bound to MD-2. Overlay of the spectra of the $^{13}CH_3$ region of [13C]LOS·MD-2 wt and F126A revealed significant chemical shift perturbation of all LOS $^{13}CH_3$ groups with the F126A mutation (Fig. 2*C* and supplemental Table S1). When the high resolution HSQC spectra of these complexes were plotted at a lower contour level, additional crosspeaks likely corresponding to minor forms of bound LOS were observed. (supplemental Fig. S1, *A* and *B*. These minor forms could be due to a reverse orientation of the lipid A backbone of the bound pseudosymmetric LOS (Fig. 2*D*) as suggested by recent molecular modeling studies of LOS·MD-2 complexes (34). Overlay of these lower contour spectra revealed that the peak positions for these minor forms were also significantly different between these two complexes, *i.e.* they experienced significant chemical shift perturbation by the F126A mutation of MD-2 (supplemental Fig. S1*C*). Phe^{126} is located in a loop adjacent to the entry of the LOS-binding pocket on MD-2. This loop has a large B-factor (17) and is mobile as shown by molecular dynamics simulation (34). The Phe^{126} side chain is completely exposed when tetraacylated LOS binds to MD-2 (an inactive complex) (15, 16). The observed significant chemical shift perturbation of the hexaacylated LOS $^{13}CH_3$ groups upon F126A mutation strongly suggests that the Phe^{126} side chain has reoriented toward the bound LOS to interact with the fatty

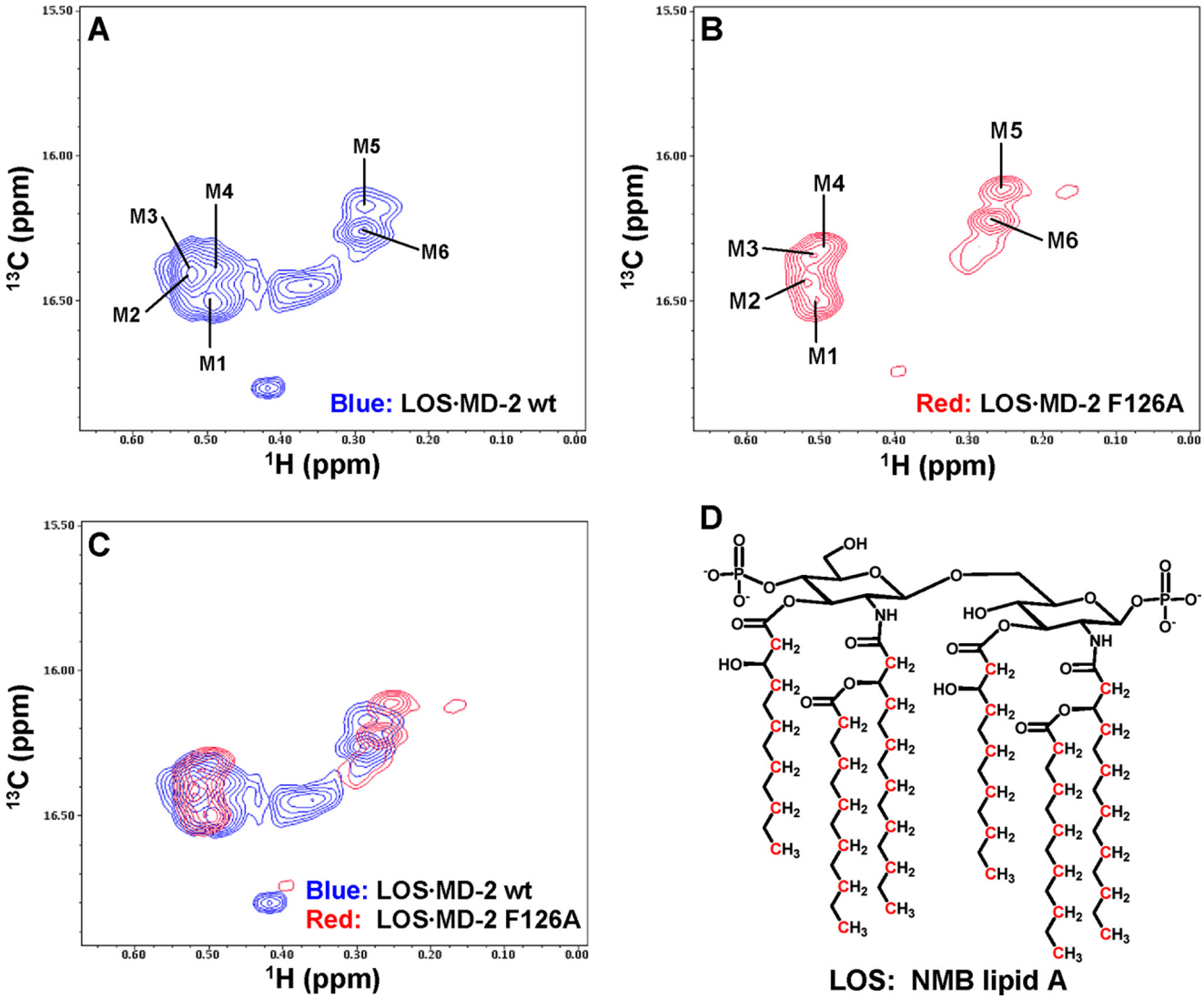

FIGURE 2. **^{13}C/^{1}H high resolution HSQC NMR spectra of the methyl region of [^{13}C]LOS·MD-2 wt and F126A.** Shown are NMR spectra of (*A*) [^{13}C]LOS·MD-2 wt complex, (*B*) [^{13}C]LOS·MD-2 F126A complex, and (*C*) overlay of the spectra in *panels A* and *B*. Sample concentrations were 240 and 260 μM for [^{13}C]LOS·MD-2 wt and [^{13}C]LOS·MD-2 F126A complex, respectively. When the spectra were plotted at a high contour level (shown here), six major crosspeak signals for the fatty acyl methyl groups of bound LOS are seen. The LOS $^{13}CH_3$ crosspeaks for the predominant form are labeled M1 to M6 as shown in *panels A* and *B*. *D*, schematic drawing of a simplified lipid A structure of NMB LOS; substitutions of ethanolamine on the phosphates are not shown. ^{13}C-labeled atoms are indicated in *red*.

acyl chains and this re-orientation of the aromatic side chain in MD-2 was induced by the bound, TLR4-activating hexaacylated LOS before interaction with TLR4. The focus of additional analyses presented below is on the major form of the bound LOS.

Comparison of the crystal structures of hexaacylated LPS·MD-2·TLR4ecd and tetraacylated lipid A·MD-2·TLR4ecd complexes revealed that in the complex containing activating hexaacylated LPS, one of the six fatty acyl chains partially protrudes from the hydrophobic cavity of MD-2, permitting fatty acyl:TLR4 contacts that are apparently important in TLR4 dimerization and activation (15–17). Our ability to identify by high resolution ^{13}C/^{1}H HSQC the crosspeaks in the methyl region of LOS·MD-2 wt and F126A complexes permitted us to probe by paramagnetic relaxation enhancement (PRE), whether a single, more surface exposed fatty acyl chain is: 1) a distinguishing characteristic of TLR4-activating endotoxin (LOS)·MD-2 complexes manifest before interaction with and dimerization of TLR4 and/or 2) dependent on Phe^{126} of MD-2.

The relative surface exposure of the individual $^{13}CH_3$ groups was determined using PRE by measuring the ^{1}H T_2 relaxation rates of the LOS $^{13}CH_3$ groups in the presence and absence of a neutral chelated paramagnetic gadolinium compound Gd(DPTA-BMA) (Fig. 3*A*) (29–31). Perturbation by Gd(DPTA-BMA) reflects the relative solvent/surface accessibility of the individual fatty acyl chains (*i.e.* CH_3 groups) in LOS·MD-2 wt and F126A complexes as the less sequestered groups will be more readily affected by the paramagnetic reagent (30, 35). In both [^{13}C]LOS·MD-2 wt and F126A complexes, five of the ^{13}C/^{1}H LOS methyl crosspeaks (M2-M6) showed similar PRE rates (Fig. 3*B*) indicating that the methyl groups have similar distances from their respective atomic coordinates to the protein surface of MD-2. However, one (M1) methyl signal in each complex had more significant PRE effects

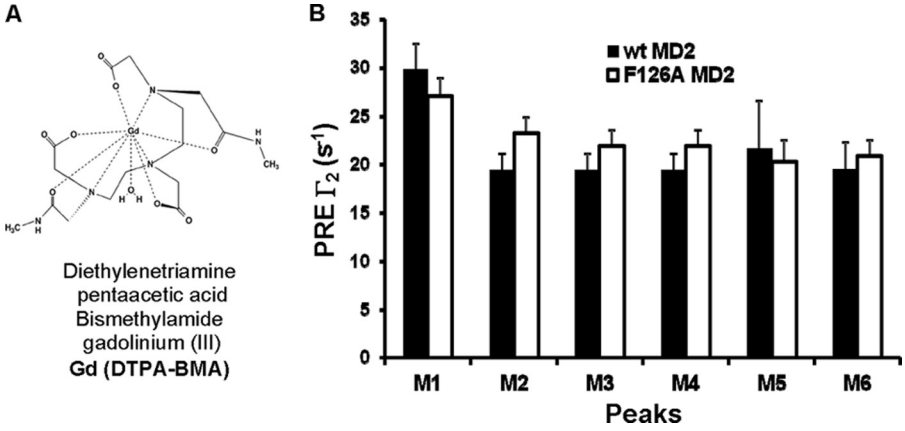

FIGURE 3. **Sensitivity of the LOS methyl signals of [^{13}C]LOS·MD-2 wt and F126A complexes to paramagnetic relaxation.** *A*, structure of the neutral chelating gadolinium paramagnetic agent Gd(DPTA-BMA). *B*, plot of paramagnetic relaxation enhancement (PRE) Γ_2 *versus* LOS $^{13}CH_3$ peaks M1-M6. To determine the relative solvent/surface exposure of the individual $^{13}CH_3$ signals from each of the six lipid A fatty acyl chains, ^{1}H T_2 relaxation data of the LOS $^{13}CH_3$ were acquired for the individual [^{13}C]LOS·MD-2 wt and F126A complexes in the absence and presence of 4 mM Gd(DTPA-BMA). The PRE rates, Γ_2, were calculated by subtracting the diamagnetic relaxation rates $R_{2,dia}$ (obtained in the absence of the paramagnetic agent) from the paramagnetic relaxation rates $R_{2,para}$ (obtained in the presence of the paramagnetic agent) and by using data collected with ^{1}H T_2 Carr-Purcell-Meiboom-Gill (CMPG) delays of 0.92 and 14.71 ms as previously described (29). Peak names correlate with the crosspeak labels shown in Fig. 2. Sample concentrations were 240 and 260 μM for [^{13}C]LOS·MD-2 wt and [^{13}C]LOS·MD-2 F126A, respectively. A concentrated stock solution of Gd(DTPA-BMA) was used to minimize the change in [^{13}C]LOS·MD-2 concentration upon addition of the reagent.

(Fig. 3*B*) suggesting that the $^{13}CH_3$ group of this fatty acyl chain was less sequestered and more solvent/surface accessible, *i.e.* protruding out of the hydrophobic pocket of both wt and F126A MD-2, independent of LOS·MD-2 association with TLR4. These findings suggest that protrusion of one of the six fatty acyl chains is a feature of monomeric complexes of hexaacylated lipid A/endotoxin (LOS) with MD-2 that precedes interactions of this complex with TLR4. The apparent similarity of this property in LOS·MD-2 wt and F126A complexes suggests that protrusion of a single fatty acyl chain of LOS bound to MD-2 is not dependent on Phe^{126} and so not sufficient for TLR4 activation.

Monomeric Ternary Complexes of [^{13}C]LOS·MD-2·TLR4ecd—According to current theory, TLR4 activation by hexaacylated endotoxin is driven by dimerization of two hexaacylated lipid A/endotoxin·MD-2·TLR4 ternary complexes. The corresponding monomers of the TLR4-activating ternary complexes must have distinguishing structural features from ternary complexes that do not trigger TLR4 dimerization and activation (*e.g.* LOS·MD-2 F126A·TLR4). To test if these distinguishing structural features include differences in the positioning of the fatty acyl chains of bound hexaacylated endotoxin in the ternary complex, the same LOS·MD-2 wt and F126A complexes analyzed by NMR were used to produce and purify ternary complexes with soluble TLR4ecd for subsequent NMR analysis. TLR4ecd was expressed in insect cells as a stable, secreted N-terminal His_6-tagged protein and purified from conditioned insect medium by a combination of metal chelation and size exclusion chromatography. The latter chromatographic step showed that the purified TLR4ecd was exclusively a monomer (Fig. 4*A*). Reaction of TLR4ecd with either LOS·MD-2 complex described above resulted in the generation of a radiolabeled complex that migrated with M_r ~100,000 as determined by size exclusion on Sephacryl S300 consistent with a monomer of the trimer LOS·MD-2·TLR4ecd (Fig. 4*B*). The concentration and functional activity of TLR4ecd was monitored analytically by size exclusion chromatography throughout the purification to assess reactivity with radiolabeled [^{3}H]LOS·MD-2 (25,000 cpm/pmol). Nearly complete conversion of [^{3}H]LOS·MD-2, wt or F126A, to [^{3}H]LOS·MD-2·TLR4ecd was observed following the reaction of 0.8–1 nM [^{3}H]LOS·MD-2 with the purified TLR4ecd, indicating pM reactivity of monomeric TLR4ecd with monomeric endotoxin·MD-2 (Fig. 4*B*).

Prior to reaction with [^{13}C]LOS·MD-2, ^{13}C/^{1}H HMQC, and HSQC NMR spectra were collected on the concentrated sample of TLR4ecd to ensure that any crosspeaks detected due to the ^{13}C natural abundance of the purified TLR4ecd did not overlap with [^{13}C]LOS signals. As shown in supplemental Fig. S2, the crosspeaks derived from both the methyl (CH_3) and methylene (CH_2) groups of [^{13}C]LOS were clearly resolved from signals due to ^{13}C natural abundance of the purified TLR4ecd.

A molar excess (1.2×) of concentrated TLR4ecd was incubated with [$^{13/14}$C]LOS·MD-2 (wt and F126A) for 30 min at 37 °C. Complete conversion of [$^{13/14}$C]LOS·MD-2 to [$^{13/14}$C]-LOS·MD-2·TLR4ecd was verified by Sephacryl S300 size exclusion chromatography (Fig. 4*C*). Comparison of ^{13}C/^{1}H HSQC spectra of the binary [^{13}C]LOS·MD-2 and ternary [^{13}C]LOS·MD-2·TLR4ecd complexes containing wt or F126A MD-2 (Fig. 5, *A* and *B*) revealed a significant chemical shift perturbation upon TLR4ecd binding for all $^{13}CH_3$ groups of LOS bound to MD-2. More severe and selective line broadening was observed for LOS M1-M4 $^{13}CH_3$ groups, which includes the $^{13}CH_3$ group M1 that protrudes out of the LOS-binding pocket of MD-2. Overlay of the ^{13}C/^{1}H high resolution HSQC spectra of the two ternary complexes (Fig. 5*C*) showed chemical shift perturbation of the LOS $^{13}CH_3$ groups by the F126A mutation of MD-2 in the LOS·MD-2 F126A·TLR4ecd ternary complex, consistent with the essential role of Phe^{126} in the TLR4-activating properties of the LOS·MD-2·TLR4 complex.

Comparison of ^{13}C/^{1}H HMQC NMR spectra of the binary [^{13}C]LOS·MD-2 *versus* the ternary [^{13}C]LOS·MD-2 wt·TLR4ecd complexes showed a remarkable broadening of the

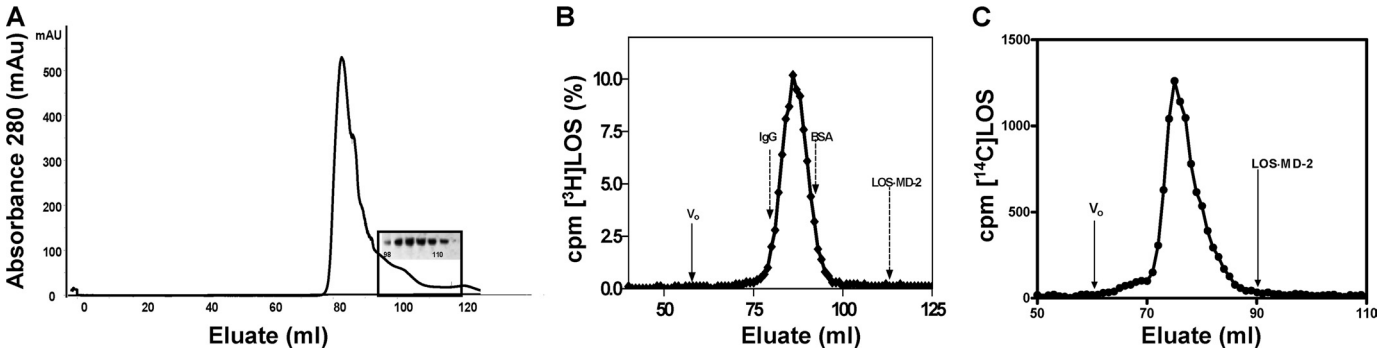

FIGURE 4. **Isolation of TLR4ecd, evaluation of reactivity with LOS·MD-2, and preparation of LOS·MD-2·TLR4ecd complexes.** *A*, monomeric His_6TLR4ecd was isolated on Sephacryl S200 (1.6 cm × 100 cm) at 4 °C at a flow rate of 0.5 ml/min in 20 mM phosphate, 150 mM NaCl, 0.005% BSA, pH 7.1 after application of the concentrated imidazole eluate fractions that contained His_6TLR4ecd recovered from the Ni FF Sepharose column. Fractions (2 ml) from the Sephacryl S200 were collected and tested for immunoreactivity with an anti-His antibody; a blot of fractions containing His_6TLR4ecd is shown. *B*, the reactivity of the purified TLR4ecd (5 μl of the S200 peak) was evaluated by reaction with [^{3}H]LOS·MD-2 (1.1 nM) in PBS, pH 7.4. Samples were incubated in 0.5 ml for 15 min at 37 °C and reaction products were resolved on S300 Sephacryl (1.6 cm × 70 cm) in PBS, 0.1% HSA, pH 7.4. Radioactivity in eluate fractions was determined by liquid scintillation spectroscopy. The experiment shown is a representative chromatogram; elution peaks of IgG (158,000), BSA (65,000), and LOS·MD-2 (25,000) are indicated. *C*, molar excess (1.2×) of purified TLR4ecd was incubated with [$^{13/14}$C]LOS·MD-2 wt or F126A for 30 min at 37 °C; an aliquot of the reaction mixture was analyzed by size exclusion on Sephacryl S300 equilibrated in 20 mM phosphate, 150 mM NaCl, pH 7.1. The amount of radioactivity in each fraction was evaluated by liquid scintillation spectroscopy. The data shown here are representative of multiple similar experiments ($n > 4$).

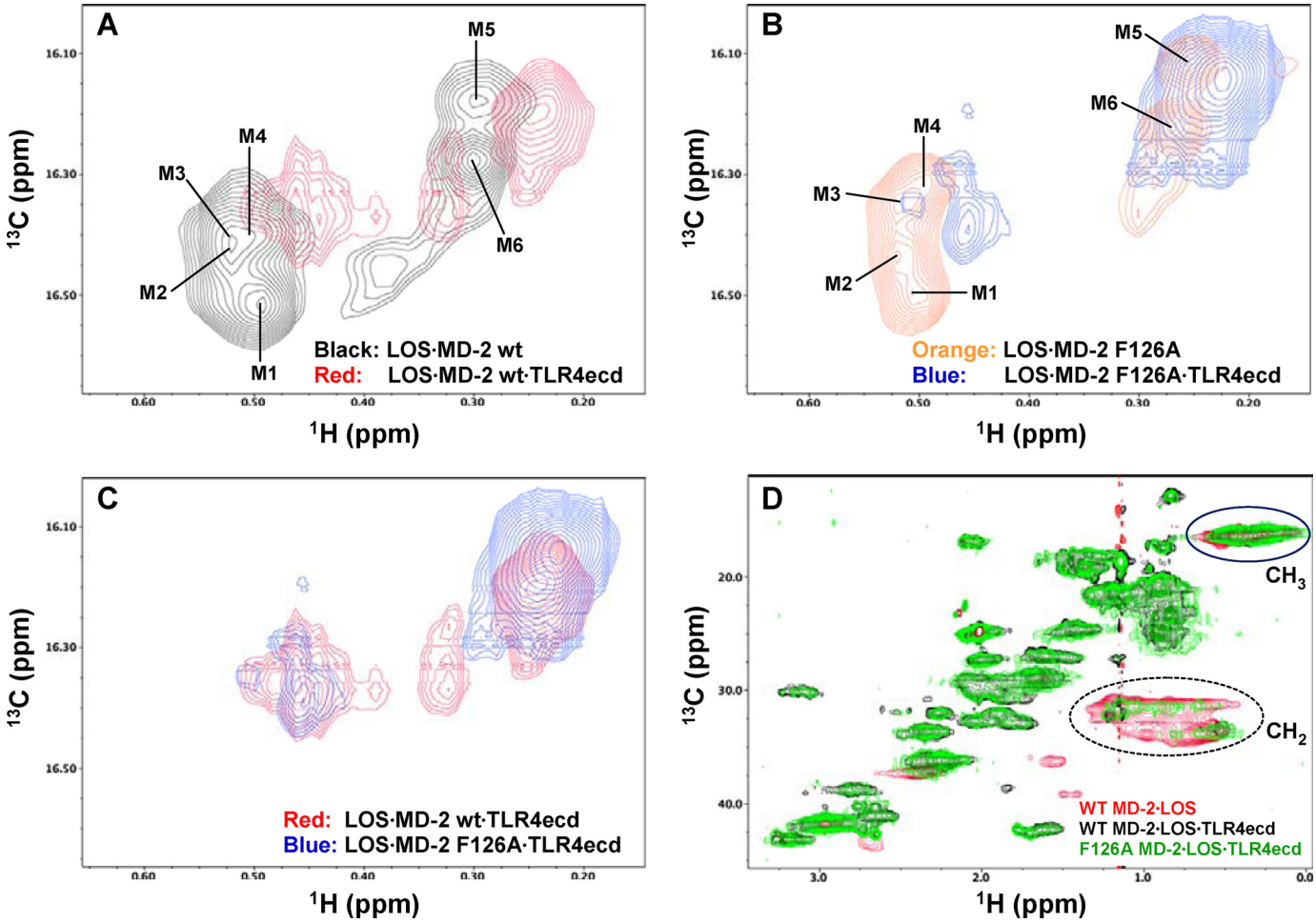

FIGURE 5. **Comparison of the ^{13}C/^{1}H HSQC and HMQC NMR spectra of [^{13}C]LOS in LOS·MD-2 wt and F126A binary complexes with their respective LOS·MD-2·TLR4ecd ternary complexes.** High resolution HSQC spectra of the LOS $^{13}CH_3$ region were overlaid for (*A*)[^{13}C]LOS·MD-2 wt binary complex in *black* and [^{13}C]LOS·MD-2 wt·TLR4ecd ternary complex in *red*, *B*, [^{13}C]LOS·MD-2 F126A binary complex in *orange*, and [^{13}C]LOS·MD-2 F126A·TLR4ecd ternary complex in *blue*, (*C*) [^{13}C]LOS·MD-2 wt·TLR4ecd ternary complex in *red*, and [^{13}C]LOS·MD-2 F126A·TLR4ecd ternary complex in *blue*. The LOS $^{13}CH_3$ crosspeaks corresponding to the major form of bound LOS are labeled as M1-M6 as shown in *panels A* and *B*. *D*, HMQC spectral overlay of [^{13}C]LOS·MD-2 wt binary complex in *red*, [^{13}C]LOS·MD-2 wt·TLR4ecd ternary complex in *black*, and [^{13}C]LOS·MD-2 F126A·TLR4ecd ternary complex in *green*. The sample concentrations were 90, 110, and 85 μM for [^{13}C]LOS·MD-2 wt, [^{13}C]LOS·MD-2 wt·TLR4ecd, and [^{13}C]LOS·MD-2 F126A·TLR4ecd complexes, respectively. NMR crosspeaks corresponding to the LOS methyl ($^{13}CH_3$) and methylene ($^{13}CH_2$) regions are circled in the figure. The LOS methylene ($^{13}CH_2$) crosspeaks were significantly reduced in intensity, particularly in the [^{13}C]LOS·MD-2 wt·TLR4ecd ternary complex. An enlarged version of the methylene region of (*D*) at a lower contour level (to the spectral floor noise level) and with a different color scheme is represented in supplemental Fig. S3.

signals derived from the $^{13}CH_2$ (methylene) groups of LOS fatty acyl chains, especially in the ternary complex containing wt MD-2 (Fig. 5*D* and supplemental Fig. S3). These changes were not due to dissociation of [^{13}C]LOS from the ternary complex or multimerization of these complexes. After NMR analyses, the complexes were re-examined by size exclusion chromatography. The post-NMR and pre-NMR elution profiles were identical for all complexes. These subtle differences in line broadening of the LOS-derived $^{13}CH_2$ signals in the wt *versus* F126A MD-2 containing ternary complexes could reflect differential ligand dynamics in these complexes due to the mutation of Phe^{126}.

DISCUSSION

Lipid A acyl chains of endotoxin bound to MD-2 were analyzed by NMR using unique reagents comprised of TLR4-activating or -inhibiting endotoxin·MD-2 complexes containing ^{13}C-labeled endotoxin bound either to wt or F126A MD-2, respectively. [^{13}C]Endotoxin, in which each of the lipid A fatty acyl chains of all LOS molecules contained a terminal $^{13}CH_3$ group followed by alternating [^{12}C] and [^{13}C] atoms, was obtained by metabolic labeling of endotoxin (LOS) with [1-^{12}C], [2-^{13}C]acetate. The bacterial mutant (NMB Ace1) utilized labeled acetate added to the growth medium as the source of essentially all acetyl precursors needed for fatty acid synthesis (24, 25). The stability of sMD-2 in insect cell medium and its reactivity with monomeric endotoxin·albumin complexes permitted the generation of monomeric endotoxin·MD-2 complexes in high yield (26). The remarkable stability of these monomeric endotoxin·MD-2 complexes allowed the purification and subsequent concentration of the complexes as needed for NMR analyses. NMR revealed discrete differences in the ^{13}C/^{1}H high resolution HSQC spectra of the wt and F126A mutant binary LOS·MD-2 and ternary LOS·MD-2·TLR4ecd complexes. These spectra were monitored to assess the microenvironment of the fatty acyl chains upon engagement of LOS with wt or F126A MD-2 and of these binary complexes with TLR4ecd. These unique reagents and analyses have permitted us to address the following two questions raised by the observations of Park *et al.* (17): 1) Are protrusion of a single fatty acyl chain of hexaacylated endotoxin and re-orientation of the aromatic side chain of Phe^{126} intrinsic properties of TLR4-activating hexaacylated endotoxin·MD-2 complexes, apparent before contact of this complex with TLR4? 2) Does Phe^{126} affect the positioning of the acyl chains of bound endotoxin and potentially promote fatty acyl:TLR4 contacts apparently needed for TLR4 activation at the dimerization interface?

^{13}C/^{1}H high resolution HSQC spectra of the $^{13}CH_3$ groups of LOS·MD-2 wt and LOS·MD-2 F126A showed six prominent and distinct signals in each complex (Fig. 2). These six crosspeaks correspond to signals deriving from the six terminal $^{13}CH_3$ groups of the bound hexaacylated LOS and reflect the distinct microenvironment of each fatty acyl chain terminus when LOS is bound to either wt or F126A MD-2. For both wt and mutant complexes, five of the six ^{13}C/^{1}H methyl crosspeaks showed closely similar paramagnetic relaxation enhancement (PRE) (Fig. 3), a measure of solvent/surface accessibility. One methyl group (M1) in both complexes was more susceptible to quenching (*i.e.* a larger PRE rate) by Gd(DPTA-BMA), indicating that this fatty acyl chain is less sequestered and presumably protruding out of the hydrophobic pocket of both wt and F126A MD-2 complexes. These findings suggest that protrusion of one of six fatty acyl chains of hexaacylated endotoxin bound to MD-2 is a structural hallmark of hexaacylated endotoxin (lipid A)·MD-2 binary complexes, independent of and preceding interactions with TLR4. Both the geometry of fatty acyl chain substitution and the length of the fatty acyl chains differ between the TLR4-activating *Escherichia coli* LPS used in the crystal structure studies of Park *et al.* (17) and the TLR4-activating meningococcal LOS used in these studies (Fig. 2*D*). Therefore, consistent with the "pattern recognition" properties of MD-2 and TLR4, the protrusion of one of six fatty acyl chains of bound TLR4-activating endotoxin from MD-2 does not depend on a single structural composition of lipid A. Studies are in progress, following the analytic approaches described here, to further define the structural requirements for this property of endotoxin (lipid A)·MD-2 complexes and its relation to TLR4 activation.

As indicated, ^{13}C/^{1}H high resolution HSQC spectra of LOS bound to F126A MD-2 also showed one methyl group of six that was more susceptible to PRE by Gd(DPTA-BMA), *i.e.* less sequestered by MD-2. Since LOS·MD-2 F126A acts as a TLR4 antagonist rather than an agonist, this finding strongly suggests that exposure of a fatty acyl chain outside of the MD-2 pocket is not sufficient for TLR4 activation. Overlay of the ^{13}C/^{1}H HSQC spectra of wt and F126A complexes demonstrated differences in each $^{13}CH_3$ group signal between the two binary complexes consistent with a distinct microenvironment of each fatty acyl chain terminus when LOS was bound to wt *versus* F126A MD-2. Although some of the chemical shift perturbation induced by the F126A mutation in MD-2 could be due to effects of interactions of the aromatic ring of Phe126 with nearby fatty acyl chains, the crystal structure of Park *et al.* (17) suggested hydrophobic contacts between the re-oriented Phe^{126} side chain and only two of the fatty acyl chains of bound LPS. Therefore, our findings suggest a more global effect of Phe^{126} on the surrounding microenvironment of each of the fatty acyl chains of bound LOS, *i.e.* an effect on the positioning of the bound LOS as a whole.

While Phe^{126} is apparently not necessary for protrusion of a fatty acyl chain of TLR4-activating endotoxin from MD-2, Phe^{126} may be necessary to guide/anchor positioning of a fatty acyl chain(s) in a way that optimizes fatty acyl:TLR4 contacts at the dimerization interface and/or MD-2:TLR4 contacts. The significant chemical shift perturbation observed for the LOS methyl groups upon F126A mutation (Fig. 2*C* and supplemental Table S1) seems most compatible with re-orientation of the Phe^{126} side chain toward the fatty acyl chains of bound LOS within the LOS·MD-2 wt complex, suggesting that this local conformational change in MD-2 is TLR4-independent and may represent a necessary signature of TLR4-activating endotoxin·MD-2 complexes. The presence of conserved glycines on either end of the "Phe^{126} loop" is consistent with the apparent importance of the conformational mobility of this region and the ability of MD-2 to bind and confer TLR4 agonist (or antagonist) properties on an array of endotoxin species with

varying numbers, distribution, and lengths of fatty acyl chains. The flexibility of this region is reflected in the crystal structure of Park *et al.* (17) where the least resolved structure (*i.e.* region of the greatest mobility) was observed in the Phe^{126} loop between the βG and βH strands. The NMR data presented here support the conclusions of DeMarco and Woods (34) that utilized molecular dynamics simulations to predict that hexaacylated LOS or LPS bound to MD-2 in a binary complex would have one acyl chain partially accessible to solvent lying near the protein surface and that the acyl chains within the MD-2 pocket would maintain mobility.

In contrast to TLR3 which requires homodimerization to accommodate binding of dsRNA ligand (36), our findings (Fig. 4*B*) demonstrate that high affinity (pM) binding of E·MD-2 with TLR4 occurs between monomeric E·MD-2 and monomeric TLR4. Whether monomeric E·MD-2 is presented to TLR4 or an E monomer is presented to pre-assembled MD-2·TLR4, the initial product is a monomer of the ternary complex E·MD-2·TLR4. The E·MD-2·TLR4 product is the most proximal intermediate in endotoxin-induced TLR4 dimerization (*i.e.* formation of [E·MD-2·TLR4]$_2$), when it is composed of TLR4-activating hexaacylated E,wt MD-2, and TLR4 or is the final product of TLR4 antagonists when containing either underacylated E and/or mutant (*e.g.* F126A) MD-2 (15–17). For reasons not yet clear (see below), reaction of either LOS·MD-2 wt or LOS·MD-2 F126A with the insect cell-derived recombinant human TLR4ecd yielded exclusively a monomeric ternary complex whether at pM-nM concentrations or >100 μM used for NMR analyses. This is in contrast to the dimeric ternary complexes previously reported when either hexaacylated *E. coli* LPS or meningococcal LOS was complexed to human MD-2·TLR4ecd (13, 17). Since the two hexaacylated endotoxin species have closely similar MD-2·TLR4-activating properties (12) and the LOS used in earlier studies (13) was the same as that used in this study, we believe the absence of dimerization of the LOS·MD-2·TLR4ecd ternary complex observed herein reflects structural differences between the recombinant TLR4ecd used in this study *versus* the earlier studies. Structural differences between the insect cell-derived His$_6$-TLR4ecd (aa 24–631) produced in this study and the recombinant human TLR4ecd produced in earlier studies (aa 24–631 generated from a transfected HEK293 cell line (13) and aa 27–631 from insect cells (17)) that yielded dimeric ternary complexes include differences in epitope tags and the composition and extent of glycosylation correlating with an insect *versus* eukaryotic cell-derived protein. Whatever the pertinent variable(s), our findings underscore that the minimum structural requirements in TLR4 for agonist-induced TLR4 dimerization are not yet clear (37). For the purposes of this study, the exclusive formation of a monomeric ternary complex was fortuitous. It allowed us to demonstrate that pM interactions between E·MD-2 and TLR4ecd are achieved by agonist-independent interactions that occur entirely within a single ternary complex and to compare by NMR the lipid A fatty acyl chains of TLR4-activating and TLR4-inhibiting ternary complexes containing, respectively, wt and F126A MD-2.

Comparison of the ^{13}C/^{1}H HSQC and HMQC spectra of LOS in the ternary complexes containing wt *versus* F126A MD-2 (Fig. 5) showed Phe^{126}-dependent differences that could be relevant to the different functional properties of these complexes. In both complexes, the engagement of TLR4 resulted in an apparent re-orientation of the fatty acyl chains since the acyl methyl groups overall underwent significant chemical shift perturbations both in position and linewidth of the signal. As indicated by the selective line broadening of the LOS methyl crosspeaks (Fig. 5, *A* and *B*) and loss of LOS methylene signals from the acyl chains, particularly in the wt MD-2·LOS·TLR4ecd ternary complex (Fig. 5*D*), the effect of TLR4 association was more pronounced overall on the wt MD-2 complex than in the F126A mutant complex. Although some of these changes could reflect altered tumbling properties of the ternary (M_r ~100,000) *versus* the binary (M_r ~25,000) complexes, the fact that these changes were more pronounced in the ternary complex containing wt MD-2 and included changes in the chemical shift of the major crosspeaks of the $^{13}CH_3$ groups suggests a further re-arrangement of the LOS fatty acyl chains within the TLR4-activating ternary complex that could be functionally important.

In summary, our findings demonstrate that Phe^{126} of MD-2 affects the position and surrounding environment of the bound fatty acyl chains of TLR4-activating hexaacylated endotoxin. These effects of Phe^{126} are manifest before interactions with TLR4 and are likely driven by hydrophobic interactions between the fatty acyl chains of the bound endotoxin and the aromatic side chain of Phe^{126}. Phe^{126} acts as a "hydrophobic switch" driving agonist-dependent recognition of TLR4-activating E·MD-2 by promoting formation of an agonist-dependent composite binding surface made up of optimally extruded endotoxin fatty acyl chain and an altered MD-2 surface conferred by re-arrangement of the Phe^{126} loop.

Acknowledgments—We thank Dr. Klaus Zangger, Institute of Chemistry/Organic and Bioorganic Chemistry University of Graz, Graz, Austria for the generous gift of the purified Gd(DPTA-BMA).

REFERENCES

1. Beutler, B., and Rietschel, E. T. (2003) Innate immune sensing and its roots: the story of endotoxin. *Nat. Rev. Immunol.* **3,** 169–176
2. Miller, S. I., Ernst, R. K., and Bader, M. W. (2005) LPS, TLR4, and infectious disease diversity. *Nat. Rev. Microbio.l* **3,** 36–46
3. Gioannini, T. L., Teghanemt, A., Zhang, D., Levis, E. N., and Weiss, J. P. (2005) Monomeric endotoxin:protein complexes are essential for TLR4-dependent cell activation. *J. Endotoxin Res.* **11,** 117–123
4. Miyake, K. (2003) Innate recognition of lipopolysaccharide by CD14 and toll-like receptor 4-MD-2: unique roles for MD-2. *Int. Immunopharmacol.* **3,** 119–128
5. Ulevitch, R. J., and Tobias, P. S. (1999) Recognition of gram-negative bacteria and endotoxin by the innate immune system. *Curr. Opin. Immuno.l* **11,** 19–22
6. Akira, S. (2009) Pathogen recognition by innate immunity and its signaling. *Pro.c Jpn. Acad. Ser. B. Phys. Bio.l. Sc.i* **85,** 143–156
7. Fitzgerald, K. A., and Chen, Z. J. (2006) Sorting out Toll signals. *Cell* **125,** 834–836
8. Kawai, T., and Akira, S. (2010) The role of pattern-recognition receptors in innate immunity: update on Toll-like receptors. *Na.t Immunol.* **11,** 373–384
9. Ostuni, R., Zanoni, I., and Granucci, F. (2010) Deciphering the complexity of Toll-like receptor signaling. *Cell Mol. Life Sc.i* **67,** 4109–4134
10. Yamamoto, M., and Akira, S. (2009) Lipid A receptor TLR4-mediated signaling pathways. *Adv. Exp. Med. Biol.* **667,** 59–68

11. Meng, J., Gong, M., Bjorkbacka, H., and Golenbock, D. T. (2011) Genome-wide expression profiling and mutagenesis studies reveal that lipopolysaccharide responsiveness appears to be absolutely dependent on TLR4 and MD-2 expression and is dependent upon intermolecular ionic interactions. *J. Immunol.* **187,** 3683–3693
12. Gioannini, T. L., Teghanemt, A., Zhang, D., Coussens, N. P., Dockstader, W., Ramaswamy, S., and Weiss, J. P. (2004) Isolation of an endotoxin-MD-2 complex that produces Toll-like receptor 4-dependent cell activation at picomolar concentrations. *Proc. Natl. Acad. Sci. U.S.A.* **101,** 4186–4191
13. Prohinar, P., Re, F., Widstrom, R., Zhang, D., Teghanemt, A., Weiss, J. P., and Gioannini, T. L. (2007) Specific high affinity interactions of monomeric endotoxin.protein complexes with Toll-like receptor 4 ectodomain. *J. Biol. Chem.* **282,** 1010–1017
14. Teghanemt, A., Zhang, D., Levis, E. N., Weiss, J. P., and Gioannini, T. L. (2005) Molecular basis of reduced potency of underacylated endotoxins. *J. Immuno.l* **175,** 4669–4676
15. Kim, H. M., Park, B. S., Kim, J. I., Kim, S. E., Lee, J., Oh, S. C., Enkhbayar, P., Matsushima, N., Lee, H., Yoo, O. J., and Lee, J. O. (2007) Crystal structure of the TLR4-MD-2 complex with bound endotoxin antagonist Eritoran. *Cell* **130,** 906–917
16. Ohto, U., Fukase, K., Miyake, K., and Satow, Y. (2007) Crystal structures of human MD-2 and its complex with antiendotoxic lipid IVa. *Science* **316,** 1632–1634
17. Park, B. S., Song, D. H., Kim, H. M., Choi, B. S., Lee, H., and Lee, J. O. (2009) The structural basis of lipopolysaccharide recognition by the TLR4-MD-2 complex. *Nature* **458,** 1191–1195
18. Resman, N., Vasl, J., Oblak, A., Pristovsek, P., Gioannini, T. L., Weiss, J. P., and Jerala, R. (2009) Essential roles of hydrophobic residues in both MD-2 and toll-like receptor 4 in activation by endotoxin. *J. Biol. Chem.* **284,** 15052–15060
19. Gruber, A., Mancek, M., Wagner, H., Kirschning, C. J., and Jerala, R. (2004) Structural model of MD-2 and functional role of its basic amino acid clusters involved in cellular lipopolysaccharide recognition. *J. Biol. Chem.* **279,** 28475–28482
20. Walsh, C., Gangloff, M., Monie, T., Smyth, T., Wei, B., McKinley, T. J., Maskell, D., Gay, N., and Bryant, C. (2008) Elucidation of the MD-2/TLR4 interface required for signaling by lipid IVa. *J. Immunol.* **181,** 1245–1254
21. Kawasaki, K., Nogawa, H., and Nishijima, M. (2003) Identification of mouse MD-2 residues important for forming the cell surface TLR4-MD-2 complex recognized by anti-TLR4-MD-2 antibodies, and for conferring LPS and taxol responsiveness on mouse TLR4 by alanine-scanning mutagenesis. *J. Immunol.* **170,** 413–420
22. Teghanemt, A., Re, F., Prohinar, P., Widstrom, R., Gioannini, T. L., and Weiss, J. P. (2008) Novel roles in human MD-2 of phenylalanines 121 and 126 and tyrosine 131 in activation of Toll-like receptor 4 by endotoxin. *J. Biol. Chem.* **283,** 1257–1266
23. Kobayashi, M., Saitoh, S., Tanimura, N., Takahashi, K., Kawasaki, K., Nishijima, M., Fujimoto, Y., Fukase, K., Akashi-Takamura, S., and Miyake, K. (2006) Regulatory roles for MD-2 and TLR4 in ligand-induced receptor clustering. *J. Immunol.* **176,** 6211–6218
24. Giardina, P. C., Gioannini, T., Buscher, B. A., Zaleski, A., Zheng, D. S., Stoll, L., Teghanemt, A., Apicella, M. A., and Weiss, J. (2001) Construction of acetate auxotrophs of Neisseria meningitidis to study host-meningococcal endotoxin interactions. *J. Biol. Chem.* **276,** 5883–5891
25. Post, D. M., Zhang, D., Weiss, J. P., and Gibson, B. W. (2006) Stable isotope metabolic labeling of *Neisseria meningitidis* lipooligosaccharide. *J. Endotoxin Res.* **12,** 93–98
26. Esparza, G. A., Teghanemt, A., Zhang, D., Gioannini, T. L., and Weiss, J. P. (2012) Endotoxin:albumin complexes transfer endotoxin monomers to MD-2 resulting in activation of TLR4. *Innate Immun.*, in press
27. Teghanemt, A., Widstrom, R. L., Gioannini, T. L., and Weiss, J. P. (2008) Isolation of monomeric and dimeric secreted MD-2. Endotoxin.sCD14 and Toll-like receptor 4 ectodomain selectively react with the monomeric form of secreted MD-2. *J. Biol. Chem.* **283,** 21881–21889
28. Lewis. K. E., and Saarinen, T. (1992) Pure absorption gradient enhanced heteronuclear single quantum correlation spectroscopy with improved sensitivity. *J. Am. Chem. Soc.* **114,** 10663–10665
29. Iwahara, J., Tang, C., and Marius Clore, G. (2007) Practical aspects of (1)H transverse paramagnetic relaxation enhancement measurements on macromolecules. *J. Magn. Reson.* **184,** 185–195
30. Pintacuda, G., and Otting, G. (2002) Identification of protein surfaces by NMR measurements with a pramagnetic Gd(III) chelate. *J. Am. Chem. Soc.* **124,** 372–373
31. Respondek, M., Madl, T., Göbl, C., Golser, R., and Zangger, K. (2007) Mapping the orientation of helices in micelle-bound peptides by paramagnetic relaxation waves. *J. Am. Chem. Soc.* **129,** 5228–5234
32. Delaglio, F., Grzesiek, S., Vuister, G. W., Zhu, G., Pfeifer, J., and Bax, A. (1995) NMRPipe: a multidimensional spectral processing system based on UNIX pipes. *J. Biomol. NMR* **6,** 277–293
33. Johnson, B. A., and Blevins, R. A. (1994) NMR View: A computer program for the visualization and analysis of NMR data. *J. Biomol. NMR* **4,** 603–614
34. DeMarco, M. L., and Woods, R. J. (2011) From agonist to antagonist: structure and dynamics of innate immune glycoprotein MD-2 upon recognition of variably acylated bacterial endotoxins. *Mol. Immuno.l* **49,** 124–133
35. Madl, T., Bermel, W., and Zangger, K. (2009) Use of relaxation enhancements in a paramagnetic environment for the structure determination of proteins using NMR spectroscopy. *Angew. Chem. Int. Ed. Engl.* **48,** 8259–8262
36. Wang, Y., Liu, L., Davies, D. R., and Segal, D. M. (2010) Dimerization of Toll-like receptor 3 (TLR3) is required for ligand binding. *J. Biol. Chem.* **285,** 36836–36841
37. Panter, G., and Jerala, R. (2011) The ectodomain of the Toll-like receptor 4 prevents constitutive receptor activation. *J. Biol. Chem.* **286,** 23334–23344